Ecological Modelling 392 (2019) 38–51

Contents lists available at ScienceDirect

Ecological Modelling

journal homepage: www.elsevier.com/locate/ecolmodel

Applicability of a one-dimensional coupled ecological-hydrodynamic numerical model to future projections in a very deep large lake (Lake Maggiore, Northern Italy/Southern Switzerland)

Andrea Fenocchi[a,*], Michela Rogora[b], Giuseppe Morabito[b,1], Aldo Marchetto[b], Stefano Sibilla[a], Claudia Dresti[b]

[a] Department of Civil Engineering and Architecture, University of Pavia, Via Ferrata 3, 27100 Pavia, Italy
[b] CNR – Water Research Institute, Largo Tonolli 50, 28922 Verbania Pallanza, Italy

ARTICLE INFO

Keywords:
1D coupled ecological-hydrodynamic model
Long-term calibration/validation
Deep-water chemistry
Phytoplankton succession
Ecosystem evolution
Climate change effects

ABSTRACT

One-dimensional coupled ecological-hydrodynamic numerical models of lakes require extensive calibration of their chemical and biological parameters. Application of these models to future projections relies on the time invariance of the calibrated model parameters and of the adopted schematisation. This is mere speculation for real ecosystems, so that it is relevant to explore the limits of coupled models over extended periods. To date, almost all applications in literature have been calibrated over a couple of years at most, with comparable validation periods, if present. Furthermore, past studies mostly concerned shallow to moderately deep small lakes, so that reproducing the hypolimnetic chemical evolution of very deep large lakes has generally been overlooked. Last, most works did not compare with observations or even model the succession of phytoplankton species, but only dealt with total Chlorophyll-*a*. Here, the GLM-AED2 (General Lake Model – Aquatic EcoDynamics) coupled model was calibrated and validated for an overall 16.75-year period for the 370-m deep and 213-km^2 wide Lake Maggiore (Northern Italy/Southern Switzerland), focusing on the reproduction of both deep-water chemistry and phytoplankton biomass and succession. Despite the modelling simplifications needed for this complex basin, the resulting performances are comparable to those in literature for shallower and smaller lakes over shorter periods. Still, extreme care must be put when interpreting the results of coupled ecological-hydrodynamic models for long-term projections, especially regarding the evolution of phytoplankton.

1. Introduction

Coupled ecological-hydrodynamic numerical models are today's most advanced tools for managing the ecosystems of lakes and reservoirs, being able to reproduce the feedbacks between physics and biogeochemistry (Hamilton and Schladow, 1997). They potentially yield additional insight to that of field data for present conditions and forecast the effects of future changes (Bruce et al., 2006). Inland basins are ordinarily exposed to pollution and climate change, which alter their ecosystems both directly and through the changes in the physical dynamics, i.e. water temperatures and internal mixing. Predictions of the effects of such processes and of the relative remediation measures are increasingly needed (Trolle et al., 2012). Despite three-dimensional (3D) coupled models can solve horizontal heterogeneities from the physical (e.g. baroclinic motions) to the biological level (e.g. phytoplankton patchiness), they still are computationally burdensome, not being suited to long-term simulations. Furthermore, they require spatially distributed boundary and initial conditions, which are troublesome to obtain. Recognising that their output is horizontally averaged, one-dimensional (1D) models allow obtaining more pragmatic outcomes than 3D models (Hamilton and Schladow, 1997), with much smaller computational effort. Hence, they are the standard for long-term applications and, thus, the object of this study.

Reliability of model predictions depends on the availability of proper data for boundary and initial conditions (Marcé et al., 2010) and on the accuracy in reproducing the relevant processes at the time scale of interest (Jørgensen, 1999). The schematisation of coupled ecological-hydrodynamic models grows from the physical level to the chemical

* Corresponding author.
E-mail addresses: andrea.fenocchi@unipv.it (A. Fenocchi), michela.rogora@irsa.cnr.it (M. Rogora), aldo.marchetto@irsa.cnr.it (A. Marchetto), stefano.sibilla@unipv.it (S. Sibilla), claudia.dresti@irsa.cnr.it (C. Dresti).
[1] Deceased, 12 July 2017.

https://doi.org/10.1016/j.ecolmodel.2018.11.005
Received 4 April 2018; Received in revised form 8 November 2018; Accepted 12 November 2018
Available online 26 November 2018

and biological ones, due to the increase in involved processes (Cui et al., 2016; Gal et al., 2009). While the description of hydrodynamics is essentially complete and hence site-independent, that of biological processes is still a simplification of actual mechanisms and relies on site-specific calibration to interpret the diversity of plankton among basins (Hamilton and Schladow, 1997; Rinke et al., 2009). Establishing a general parameterisation is elusive (Romero et al., 2004), even for neighbouring lakes with the same plankton species (Burger et al., 2008; Dietzel et al., 2013). Theoretically, parameters could be obtained from field data (Gal et al., 2009), but many chemical and biological processes cannot be isolated (Özkundakci et al., 2011). Furthermore, field estimates may not lead to the best fit (Kara et al., 2012), tweaked parameters being needed to make up for the basic representation of processes (Hamilton and Schladow, 1997; Marcé et al., 2010). Time-consuming calibration is hence necessary, the use of literature values being restricted to less sensitive parameters for which reliable values from similar environments are available.

Rising schematisation leads to declining model accuracy from the physical to the chemical and biological levels (Carraro et al., 2012; Dietzel et al., 2013; Kara et al., 2012; Rigosi et al., 2011). The increasing patchiness of variables also contributes to the drop of performances (Gal et al., 2009). While horizontal temperature and salinity gradients are mostly opposed by gravity, chemical and biological variables negligibly affect water density and hence can display significant horizontal inhomogeneities (Hamilton and Schladow, 1997). The laterally averaged results of 1D models and the vertical samples could therefore deviate. Build-up of errors from underlying model levels (Carraro et al., 2012; Rigosi et al., 2011) and growing analytical uncertainties on observations (Trolle et al., 2008b) also increase inaccuracy.

The limits of models should be acknowledged when interpreting their results. Parameterisation induces stationarity, as ecosystem changes would require a new calibration or an adjustment to the schematisation (Trolle et al., 2008a, 2008b). This is particularly limiting for plankton, for which the adopted parameters are averaged over assemblages of species during the calibration period. Even if multiple functional groups are introduced, changes in the species living in the lake, in the proportions among species within single groups and in the physiology of individual species cannot be reproduced (Burger et al., 2008; Özkundakci et al., 2011; Trolle et al., 2008b). However, for management purposes only qualitative evaluations of the response of the ecosystem to external changes are needed (Gal et al., 2014; Özkundakci et. al., 2011). Nevertheless, we must make sure that the model does not drift from reality in the long term.

Calibration and independent validation over long time series would be needed to assess the predictive power of coupled ecological-hydrodynamic models (Dietzel et al., 2013; Trolle et al., 2008b), good fit of field data being far more likely over short periods (Snortheim et al., 2017). Due to lack of observations, most applications to date have been calibrated at most over a couple of years, being occasionally validated over comparable periods (Table 1). In addition, most studies concerned shallow to moderately deep lakes (Table 1), where a segregated hypolimnion, connected to surface waters only during full turnovers, is not present. Furthermore, literature applications mainly dealt with small basins (Table 1), in which the 1D hypothesis of horizontal homogeneity is more straightforward. Last, many studies did not model the seasonal succession of phytoplankton groups or did not compare the results against field data, considering only total Chlorophyll-*a* (Chl-*a*). This is due to the demanding analytics needed to characterise the sampled biomass. Including multiple functional groups does not imply a better fit of total observed phytoplankton (Shimoda and Arhonditsis, 2016), the strongest constraint being applied by the limiting nutrient on the total biomass (Mieleitner and Reichert, 2008; Mieleitner et al., 2008), which also causes errors on each class to propagate over all the others. Adopting functional groups yet allows a higher sensitivity to changing external conditions, due to the more heterogeneous parameterisation (Shimoda and Arhonditsis, 2016). The applicability of 1D coupled ecological-hydrodynamic models to future projections in very deep large lakes is therefore quite unexplored, especially regarding the evolution of deep hypolimnion chemistry and phytoplankton succession. These two aspects are the main concerns of climate change for deep lakes in temperate zones. In fact, more prominent phytoplankton blooms (Peeters et al., 2007) with predominance of cyanophytes (Jöhnk et al., 2008), hypolimnetic oxygen depletion (Rogora et al., 2018) and accumulation of nutrients in bottom waters (Salmaso, 2005) are expected to follow the higher water temperatures and drop of mixing (Fenocchi et al., 2018).

In the only long-term ecological modelling study on deep lakes familiar to us, Dietzel et al. (2013) simulated three Swiss lakes (Table 1) with a pure ecological model, assuming time-invariant seasonal mixing coefficients between epilimnion and hypolimnion. The long-term trends of chemical and biological variables were well reproduced, yet with substantial error at the intra-annual scale. A significant decrease of model performances was obtained during validation. They attributed most errors to the simplified vertical mixing. Last, they adopted single phytoplankton and zooplankton groups. We thus aim at performing a similar investigation with a coupled ecological-hydrodynamic model and multiple phytoplankton groups, to assess intra-annual dynamics reproduction and discuss the applicability to long-term studies.

In the present study, we calibrated and validated the GLM-AED2 (General Lake Model – Aquatic EcoDynamics; Hipsey et al., 2013, 2014) 1D coupled model for the 370-m deep and 213-km^2 wide Lake Maggiore (Northern Italy/Southern Switzerland), for a 16.75-year period between 1998 and 2014. In view of applying the model to climate change projections, we optimised the calibration of deep-water chemistry and of phytoplankton biomass and succession, evaluating the performances over such aspects and determining whether a single application could catch both.

2. Materials and methods

2.1. Study area and data

Lake Maggiore is a deep lake of fluvio-glacial origin at the foothills of the Southern Central Alps, its surface being shared between Italy (~80%) and Switzerland (~20%) (Fig. 1). The lake drains the upstream watershed of River Ticino, its only outflow, including the surrounding Lakes Lugano, Orta and Varese. Lake Maggiore has 33 tributaries, the largest ones being Rivers Ticino and Toce. Miorina Dam (Fig. 1) controls its water level and ordinarily allows for a 0.5 m difference between winter and summer periods for water storage purposes. The main morphometric and hydrologic features of Lake Maggiore are listed in Table 2.

Lake Maggiore is oligomictic, full turnovers occurring only at the end of particularly cold and windy winters (Ambrosetti and Barbanti, 1999). Warming of surface temperatures (Pareeth et al., 2017) and decreasing mixing frequency (Ambrosetti and Barbanti, 1999; Rogora et al., 2018) have been observed over the last decades in response to climate change, causing relevant ecological effects (CNR-ISE, 2016; Salmaso et al., 2014). Such trends would likely continue for the rest of the 21st century (Fenocchi et al., 2018). The basin is presently oligotrophic P-limited, primary production being dominated by diatoms due to the siliceous watershed (Morabito et al., 2012). The lake suffered from eutrophication in the 1960s and 1970s, reaching the limit between mesotrophy and eutrophy (Ruggiu et al., 1998). The establishment of wastewater treatment plants and the reduction of phosphorus in detergents allowed a slow reversal to natural oligotrophy from the 1980s (Kamenir and Morabito, 2009), input nutrient loads having stabilised in the 2000s (CNR-ISE, 2016; Salmaso et al., 2014). Within the 1998–2014 study period, Lake Maggiore mixed completely with chemical homogenisation at the end of winters 1999 and 2006 (Fenocchi et al., 2018), yet partial turnovers provided hypolimnetic mixing also in 2000, 2004

Table 1
Database of considered numerical modelling literature applications compared with the present study (D-C = DYRESM-CAEDYM (1D), E-C = ELCOM-CAEDYM (3D), d. y. = disjointed years). Studies performed with the DYRESM-CAEDYM, ELCOM-CAEDYM, GLM-AED and DYRESM-WQ models listing the adopted parameters are appointed an identification letter for later referencing.

Paper		Basin	Maximum depth [m]	Surface area [km^2]	Model (dimensions)	Calibration [years]	Validation [years]
Present study		*Lake Maggiore*	*370*	*213*	*GLM-AED2 (1D)*	*8*	*7.79*
Copetti et al. (2006)	a	Lake Pusiano	25	5	D-C	1	–
Carraro et al. (2012)	b				E-C	0.88	–
Rinke et al. (2009)		Upper Lake Constance	254	473	D-C	3	–
Rinke et al. (2010)	c				D-C	3	–
Kara et al. (2012)	d	Lake Mendota	25.3	39.4	D-C	0.25	–
Snortheim et al. (2017)	e				GLM-AED (1D)	2	2
Schladow and Hamilton (1997)	f	Prospect Reservoir Prospect Reservoir	24	5.25	DYRESM-WQ (1D)	0.55	0.84
Romero et al. (2004)	g				D-C	2	–
		Lake Burragorang	90	82	D-C	2	–
					E-C	0.06	–
Bruce et al. (2006)	h	Lake Kinneret	43	170	D-C	1	1
Hillmer et al. (2008)	i				D-C, E-C	0.44	–
Gal et al. (2009)	j				D-C	6.75	–
Li et al. (2013)	k				D-C	5	–
Gal et al. (2014)	l				D-C	Future prediction only study	
Trolle et al. (2008a)	m	Lake Ravn	33	1.8	D-C	7	5
Trolle et al. (2008b)	n				D-C	7	5
Burger et al. (2008)	o	Lake Rotorua	45	79	D-C	1	2
Trolle et al. (2011)	p	Lake Okareka	33.5	3.42	D-C	3	2
		Lake Rotoehu	13.5	7.95	D-C	3	2
		Lake Ellesmere	2.5	182	D-C	3	2
Bruce et al. (2008)	q	Mono Lake	45	160	D-C	2	2
Martins et al. (2008)		Lake Verde of S. C.	21	0.9	AQUASIM (1D)	1	–
Marcé et al. (2010)	r	Lekubaso Reservoir	90	1.4	D-C	Future prediction only study	
Özkundakci et al. (2011)	s	Lake Okaro	18	0.32	D-C	2	2 × 1 d. y.
Rigosi et al. (2011)	t	El Gergal Reservoir	37	2.5	D-C	0.74	0.64
Cui et al. (2016)	u	Shahe Reservoir	14	9	D-C	2	1
Kerimoglu et al. (2017)		Lake Bourget	145	45	GOTM-FABM (1D)	5 × 1 d. y.	–
Dietzel et al. (2013)		Lower Lake Zürich	136	67.3	BELAMO (0D, pure ecological	20	10
		Walensee	151	24.19	model)	20	10
		Greifensee	32	8.45		9	10

and 2005. An extraordinary bloom of the chlorophyte *Mougeotia* occurred in summer 2011, reaching a $> 20\ g/m^3$ biomass, $1 \div 2$ orders of magnitude higher than its previous annual peaks (Stefani et al., 2016; Tapolczai et al., 2015). *Mougeotia* blooms have been happening in large deep perialpine lakes under ordinary nutrient loads, as opposed to those of cyanophytes and dinophytes, possibly as a by-product of re-oligotrophication (Tapolczai et al., 2015).

Lake Maggiore has been routinely monitored since 1981 by the Water Research Institute of the National Research Council of Italy (CNR-IRSA) of Verbania Pallanza (formerly Institute of Ecosystem Study, CNR-ISE), within the framework of the International Commission for the Protection of Italian-Swiss Waters (CIPAIS). Vertical limnological profiles have been collected at the Ghiffa site of maximum depth (Fig. 1; Table 2) with an approximate monthly frequency. Water temperature measurements and water samples for chemical analyses have been taken at depths: 0 m, 5 m, 10 m, 20 m, 30 m, 50 m, 100 m, 150 m, 200 m, 250 m, 300 m, 360 m. Integrated $0 \div 20$ m samples have been taken for phytoplankton, being analysed for total Chl-*a* concentration and the biovolumes of phytoplankton species, grouped in the six classes present in Lake Maggiore: cyanophytes, diatoms, dinophytes, chlorophytes, chrysophytes, cryptophytes. Chemical and water temperature data have also been simultaneously collected at the mouths of the 12 main tributaries (Fig. 1). Daily discharges for these streams are available, yet with several gaps for the less relevant ones.

The simulated period is the 16.75-year span between 19 January 1998 and 14 October 2014, the hydrodynamic module having been already calibrated in Fenocchi et al. (2017) over such interval, for which almost complete and validated data series are available for model feeding and evaluation. Daily series of air temperature, shortwave radiation, relative humidity, wind speed and atmospheric pressure were obtained from the Verbania Pallanza weather station, retrieving few missing radiation data from the Locarno-Monti station (Fig. 1).

2.2. Calculation of input loads

Mean monthly input loads to the model were calculated for dissolved oxygen (O_2), orthophosphate (PO_4), nitrate (NO_3), ammonium (NH_4), silica (SiO_2), dissolved organic phosphorus (DOP) and nitrogen (DON), dissolved inorganic (DIC) and organic (DOC) carbon. Incoming particulate organic phosphorus (POP), nitrogen (PON) and carbon (POC) and plankton are negligible for Lake Maggiore (Bertoni and Callieri, 1992; CNR-ISE, 2013).

Mean monthly discharges of the 12 main tributaries (Fig. 1) were employed, neglecting minor inflows, diffuse runoff and groundwater input due to the lack of data. These tributaries account for ~77% of the inflow volume during the study period. Missing monthly discharge values (10% of the total ones) were reconstructed from the discharges of the other tributaries according to hydrologic similarity, developed on a meteorological season basis to consider the different rainfall and runoff regimes during the year. Pearson correlation matrices among the mean monthly discharges of the 12 streams were built for each meteorological season. To model missing data for a tributary for a specific season, linearly regressed values from the discharges of the best correlated river for that season were adopted. In case concurrent discharges for the best correlated stream were also missing, regressed values from the second-best correlated tributary were employed, and so on, up to the third-best correlated river for the herein reconstructed data. The correlation coefficients of the adopted regressions ranged

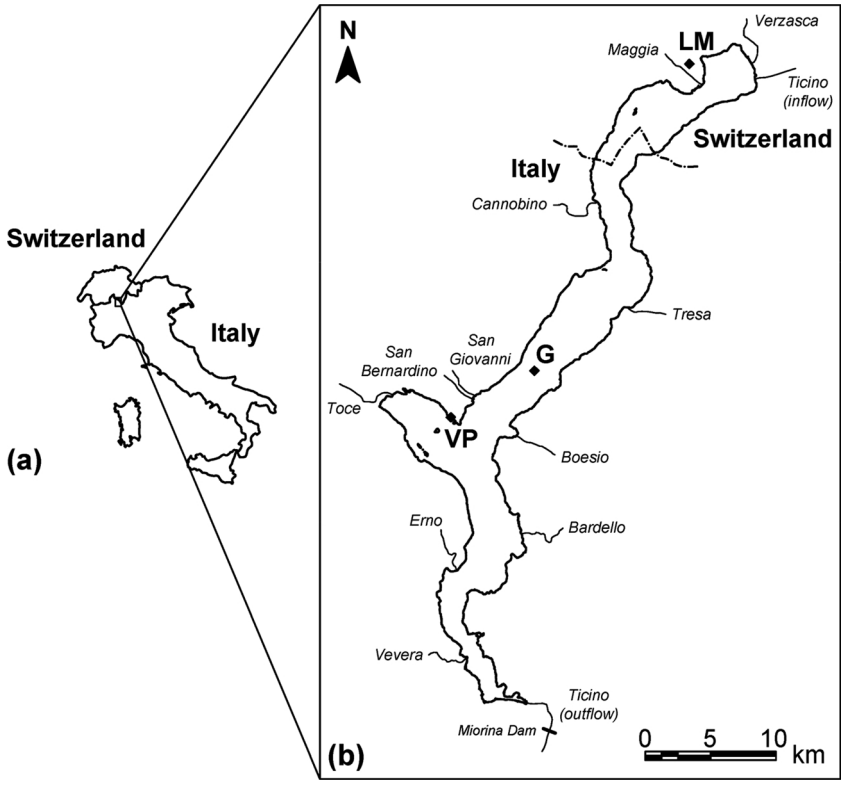

Fig. 1. Location (a) and map (b) of Lake Maggiore, displaying the final reaches of the 12 main tributaries and the employed data stations (G = Ghiffa limnological site; VP = Verbania Pallanza weather station; LM = Locarno-Monti weather station).

Table 2
Main morphometric and hydrologic features of Lake Maggiore.

Feature	Value
Surface area [km^2]	213.0
Volume [km^3]	38.1
Reference surface elevation [m a.s.l.]	193.5
Maximum depth at Ghiffa site [m]	370.0
Mean depth [m]	178.9
Watershed area [km^2]	6599.0
Mean outflowing discharge 1921-2015 [m^3/s] (CNR-ISE, 2016)	287.4
Theoretical renewal time [years]	4.2

$R = 0.39 \div 0.98$, with mean and standard deviation $\bar{R} = 0.76 \pm 0.16$ and always $p < 0.01$. Although daily discharges were available, monthly means were adopted to provide a source of averaging, partially balancing the distortion caused by the approximate monthly frequency of chemical samples. Reconstructing missing daily discharges would have also required a rainfall-runoff model of each tributary, as applying hydrologic similarity would have resulted in much lower correlation coefficients, due to the far more individual characters of watersheds at shorter time scales.

The concentrations adopted to compute mean monthly input loads were obtained as follows: 1) the sampled concentrations at the tributaries' mouths were linearly interpolated at a daily scale; 2) approximate mean monthly values were calculated from the interpolated data.

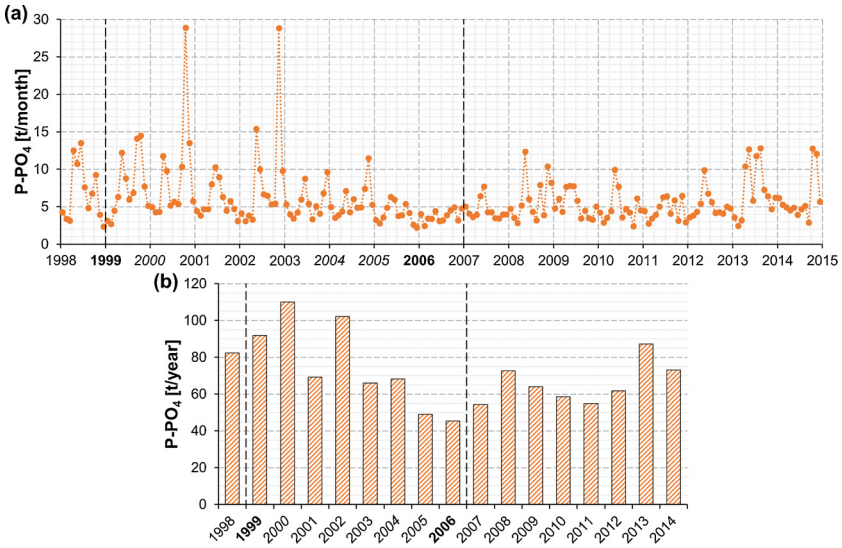

Fig. 2. Monthly (a) and annual (b) input loads of PO_4 to Lake Maggiore over 1998–2014 obtained from the overall calculated mean monthly values from the tributaries. Years with full and partial turnovers are marked in bold and italics, respectively. Model spin-up, calibration and validation periods are separated by dashed lines.

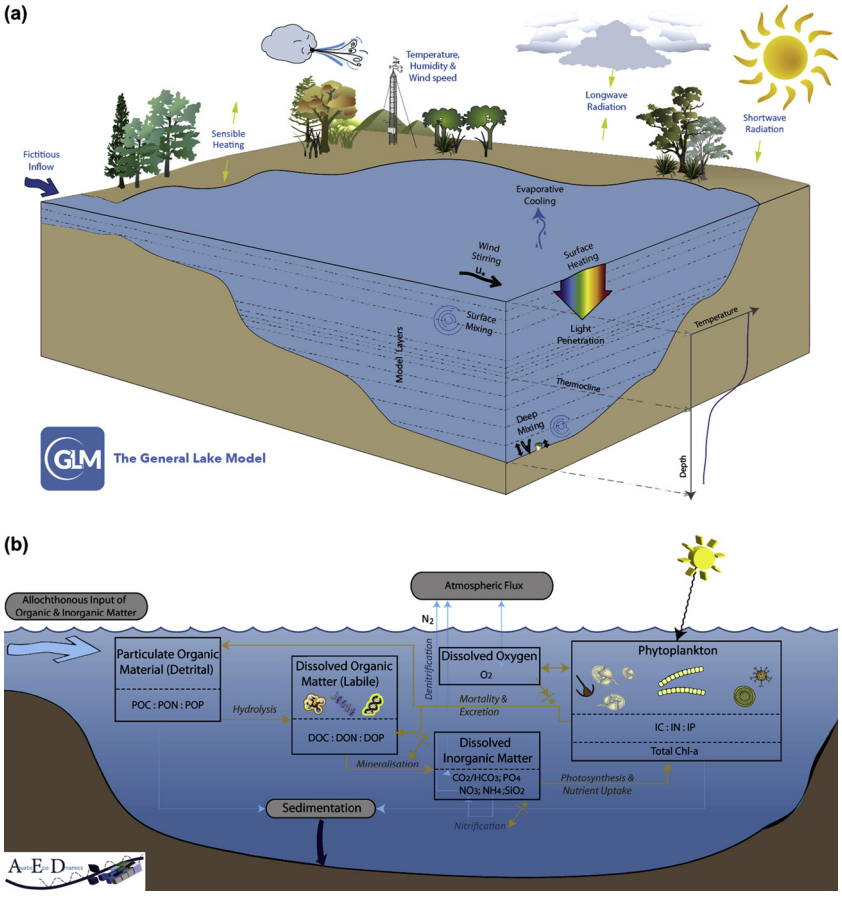

Fig. 3. Conceptual diagrams of the applied coupled model of Lake Maggiore: (a) GLM hydrodynamic module (adapted from Hipsey et al., 2014); (b) AED2 ecological module (adapted from Hipsey et al., 2013).

In the AED2 model and in the remainder of the manuscript, nutrients are expressed as concentrations and loads of their fundamental element ($P\text{-}PO_4$, $N\text{-}NO_3$, $N\text{-}NH_4$, $Si\text{-}SiO_2$). Saturation concentrations were assumed for O_2 at the tributaries due to the turbulence of lotic waters and the lack of measurements (Burger et al., 2008; Hamilton and Schladow, 1997). Saturation values were calculated with Henry's law, estimating Henry's constant as function of the atmospheric pressure recorded at Verbania Pallanza and of the sampled river water temperatures as per Sander (2015). Concentrations of DOP and DON were obtained as differences between the total (TP and TN) and the dissolved inorganic ($P\text{-}PO_4$ and $N\text{-}NO_3$ + $N\text{-}NH_4$) forms. Fig. 2 displays the overall input load series for the limiting nutrient PO_4. Peaks correspond to the 2000 and 2002 flood events.

2.3. Model setup

2.3.1. Hydrodynamic module

The General Lake Model (GLM) v2.2.0b 1D model (Hipsey et al., 2014) was employed for the hydrodynamic simulation of Lake Maggiore. The conceptual model of the present application is given in Fig. 3a. Here, in view of applying the coupled ecological-hydrodynamic model to future projections, we adopted the fixed-level enclosed-lake model configuration calibrated in Fenocchi et al. (2017). Such formulation does not consider actual inflows, outflow and direct rainfall discharges, whose inclusion over a projection study would entail a highly uncertain reconstruction of the future hydrologic regime and balance evolution (Fenocchi et al., 2018). The lake elevation is set to the reference one of Lake Maggiore (Table 2) through a calibrated input discharge that opposes daily evaporation. The model reproduces the relevant features of thermal evolution in the study period, adopting a fictitiously low light extinction coefficient to mimic the advective heat of riverine intrusions. The limits of this assumption are discussed in Fenocchi et al. (2017). The same schematisation, parameters, boundary and initial conditions used in Fenocchi et al. (2017) were retained, except for the following modifications.

A fictitious surface inflow was employed instead of a fictitious rainfall to fulfil the fixed-level constraint. This way, nutrient loads from tributaries were input at the lake surface. The employed daily inflow concentrations were obtained as follows: 1) the overall calculated mean monthly loads (e.g. Fig. 2a) were linearly interpolated at a daily scale; 2) the daily inflow concentrations were calculated as ratios between the total loads and the calibrated fictitious discharges. This modification did not impact the hydrodynamic model accuracy. Assuming input loads to always enter at the surface may be realistic for minor inflows, their momentum and buoyancy forces being rapidly damped. The main tributaries Rivers Ticino and Toce intrude at shallow depths (10 ÷ 20 m) during most of the year, sometimes reaching the surface in early spring, yet they sink to much lower depths (also > 200 m) throughout late autumn and winter (Fenocchi et al., 2017). The employed schematisation seemed however the most reasonable one given the heterogeneity of the tributaries of Lake Maggiore, spanning large rivers, natural and dammed mountain streams, creeks and outflows of smaller lakes and reservoirs, with a wide range of discharges and temperatures (Fenocchi et al., 2017), and the aim of reproducing future scenarios, in which changes in the intrusion behaviour are expected (Fenocchi et al., 2018). In the present model, nutrients are hence passed to lower layers only through vertical mixing and sinking of particulate organic matter and phytoplankton. Outflow of nutrients is not represented due to missing emissary in the model. Such approximation is suitable for Lake Maggiore due to its large surface and volume and relatively long

renewal time (Table 2), which make nutrient recycling prevalent for primary production.

The minimum and maximum thicknesses of the model layers were increased from $h_{min} = 0.1$ m to $h_{min} = 0.2$ m and from $h_{max} = 0.5$ m to $h_{max} = 2.0$ m, respectively. This was done to speed up calculations, in view of the manifold realisations needed to obtain robust statistical predictions with a Monte Carlo approach for future climate change scenarios (Fenocchi et al., 2018). This modification impacted model accuracy, requiring a slight recalibration of the light extinction coefficient from $K_d = 0.098\ m^{-1}$ to $K_d = 0.100\ m^{-1}$ and of the wind enhancement factor from $K_w = 1.15$ to $K_w = 1.14$. The final Root Mean Square Error (RMSE) and Mean Absolute Error (MAE) for water temperature over the whole depth and over separate epilimnion, metalimnion and hypolimnion are nevertheless < 10% larger than in Fenocchi et al. (2017).

2.3.2. Ecological module

The GLM model was coupled to the Aquatic EcoDynamics (AED2) ecological model (Hipsey et al., 2013). The conceptual model of the current application is illustrated in Fig. 3b. A basic NPD (Nutrients, Phytoplankton, Detritus) structure was employed. Oxygen, phosphorus, nitrogen, silica, carbon, organic matter and phytoplankton cycles were included. Mortality of phytoplankton due to grazing by zooplankton and fish was subsumed into phytoplankton respiration (Bruce et al., 2006; Burger et al., 2008; Rigosi et al., 2011; Snortheim et al., 2017). Heterotrophic bacterial respiration was captured through mineralisation of particulate (POM) and dissolved (DOM) organic matter (Bruce et al., 2006, 2008; Li et al., 2013; Snortheim et al., 2017). The contribution of macrophytes to primary production in Lake Maggiore is negligible compared to that of phytoplankton (Guilizzoni et al., 1989), as typical of large deep lakes due to the relatively restricted littoral zone (Grzybowski, 2014; Rounsefell, 1946). Nutrient release from sediments was not considered because the overlying water column was well-oxygenated in the simulated period (Rogora et al., 2018). The ecological module runs with the same hourly time step of the hydrodynamic one, allowing the resolution of photosynthesis (Bruce et al., 2006).

Phytoplankton was modelled through four functional groups, based on taxonomic classes: cyanophytes, diatoms, dinophytes and “c3phytes”, which includes chlorophytes, chrysophytes and cryptophytes. The latter group was created to reduce parameterisation, the three constituents having similar annual cycles. The employed segmentation could potentially allow reproducing the main specific features of phytoplankton in Lake Maggiore: 1) cyanophytes bloom in late summer and resist high water temperatures; 2) diatoms rapidly bloom between late winter and early spring at low temperatures and uptake silica for their shells; 3) dinophytes bloom in early summer, can withstand low phosphorus levels and have low winter survival rate; 4) c3phytes bloom in late spring (primary peak) and in early autumn (secondary peak) at tepid temperatures and survive at moderate concentrations during winter, with chrysophytes (~26% of the observed biovolume of the functional group in the study period) uptaking silica for their shells.

Fixed C:N and C:Si ratios were assumed for phytoplankton functional groups, dynamic C:P ratios being adopted only for the limiting nutrient, to which the output is most sensitive (Bruce et al., 2008; Carraro et al., 2012; Martins et al., 2008; Omlin et al., 2001). Constant C:Chl-*a* ratios were also employed for the functional groups, these being actually variable in time for each species (Kara et al., 2012; Rigosi et al., 2011). Silica uptake was activated for diatoms and c3phytes. Photoinhibition and N-fixation were not simulated.

As the calibrated K_d value is artificial, feedback of bio-turbidity on the light extinction coefficient was not considered, as the resulting alterations would have triggered non-linear effects. Rinke et al. (2010) observed that adopting a variable K_d rather than a constant one resulted in surface temperature differences in the order of ± 1 °C for simulations of Lake Constance (Germany/Switzerland/Austria), even under altered trophic status. These are much lower than the expected warming over the 21st century (Fenocchi et al., 2018). A proper light extinction coefficient $K_d = 0.227\ m^{-1}$ was yet considered in the phytoplankton submodule to reproduce light limitation, as resulting from the Poole and Atkins (1929) equation given the mean observed Secchi depth in the study period $\bar{SD} = 7.49$ m (Fenocchi et al., 2017).

The initial vertical profiles of chemical variables, i.e. O_2, PO_4, NO_3, NH_4, SiO_2, DOP, DON, DIC, DOC, POC, were set to piecewise linear interpolations of the sampled values on the first day of simulation, as done for water temperature (Fenocchi et al., 2017). Concentrations of dissolved organic nutrients were again calculated as DOP = TP - P-PO_4 and DON = TN - (N-NH_3 + N-NH_4), POP and PON being negligible also in Lake Maggiore (CNR-ISE, 2013b). For phytoplankton groups, initial constant concentrations equal to the observed integrated values were assumed in the sampled 0 ÷ 20 m layer, linearly decreasing to zero in the 20 ÷ 30 m layer with null phytoplankton below. The measured series of biovolumes of the functional groups were converted into the carbon concentrations needed by AED2 according to Reynolds (2006).

2.4. Ecological module calibration

The considered time span was split into calibration and validation periods, the former including the 8-year interval between 1 January 1999 and 31 December 2006 and the latter the 7.79-year one between 1 January 2007 and 14 October 2014 (Table 1). The initial 1998 year of simulation served as model spin-up, systematic inferior performances being observed in the first annual phytoplankton cycle, likely due to the approximate initial conditions.

Manual trial-and-error calibration was adopted to tune the ecological module, adjusting the parameters mostly within literature boundaries, until the fit to observations could no longer be improved appreciably. Automatic calibration techniques (Rigosi et al., 2011) still cannot be applied successfully to coupled models of deep lakes with multiple plankton groups. Defining an optimisation function including several variables at various depths would be ambiguous, huge computational resources would be needed due to the dimensions of the parameter space (Trolle et al., 2011) and convergence problems would arise because of the non-linear interactions between physics, chemistry and biology (Rigosi et al., 2011). Literature values, when applicable, were taken from the modelling studies in Table 1 employing the DYRESM-CAEDYM, ELCOM-CAEDYM, GLM-AED and DYRESM-WQ coupled models, which share the schematisation and main algorithms with GLM-AED2, to be sure that parameters have the same meaning. Adopting a literature value for a parameter did not imply that the latter was omitted from the calibration process, as multiple published values were tested. Due to the many variables, compromises to the fit of single ones had to be made for the sake of overall model performances. Resulting errors were compared with published ones to state their acceptability.

Model fit of chemical variables was optimised in the deep hypolimnion, i.e. in the 200 ÷ 370 m layer, being the predictability of the long-term evolution in this layer one of the research aims. Furthermore, chemical processes are more properly calibrated in the deep hypolimnion, being most isolated from the biological and physical ones. Sample results are also given for the epilimnetic 0 ÷ 20 m layer. For chemical variables, both observations and model results were numerically integrated from the values at the sampling depths. Calibrated variables were those for which extended observations were available: O_2, PO_4, NO_3, NH_4, SiO_2, DOP and DON. For phytoplankton, fit was monitored in the 0 ÷ 20 m layer of the integrated samples, numerically integrating model results at 1 m resolution. Parameters of the phytoplankton groups were calibrated to allow growth up to the observed biomasses despite excess surface nutrients, so that the obtained values reflect the adopted schematisation. Results for 0 ÷ 20 m and 200 ÷ 370 m water temperatures are also reported, numerically integrated as for the chemical variables.

Preliminary manual calibration was based on visual screening of the agreement of the trends of chemical variables and of overall quantitative equivalence and suitable succession timing for phytoplankton. Multiple goodness-of-fit metrics were employed for fine-tuning. Both the Pearson and the Spearman correlation coefficients R and R_S were considered, tested for p-value significance. The Pearson correlation coefficient measures the ability of the model to reproduce observed trends at the intra- and inter-annual scales. The Spearman correlation coefficient has a similar meaning, yet it weighs the error on the timing of fluctuations disregarding quantitative differences (Gal et al., 2009), thus being meaningful to evaluate the prediction of phytoplankton succession. The Normalised Mean Absolute Error (NMAE) and the Normalised Mean Error (NME) indices were also considered. While NMAE states the average error, NME expresses the systematic one, revealing the bias and drift effects which can be significant over long time series. The target of calibration was a compromise between maximum R and R_S and minimum NMAE and NME for each variable. The calibration process required multiple shifts between chemical and phytoplankton levels, due to the interactions between them.

Normalisation by mean observed value is standard practice for NMAE and NME. This is adequate for variables displaying small gradients and whose mean values are important to be reproduced (Kara et al., 2012), but leads to error misrepresentation when peak values are much larger than mean ones (Alewell and Manderscheid, 1998; Bruce et al., 2006). It is then inappropriate for phytoplankton, for which prominent seasonal blooms occur and the mean is biased by very small winter concentrations, and for nutrients in the epilimnion, which have much higher concentrations in winter with minimum primary production than during the rest of the year. Therefore, for fluctuating variables in the epilimnion we also normalised by the observed mean annual range ($NMAE_r$ and NME_r) in addition to by the mean value ($NMAE_m$ and NME_m).

3. Results and discussion

3.1. Model parameters

The final values of the chemical parameters resulting from the calibration and literature selection processes are listed in Table 3. Specific tuning had to be performed for 10 out of 27 chemical parameters. A very high nitrification rate and a very low denitrification rate compared to the literature range had to be used to match the very low reducing properties of Lake Maggiore waters. These are due to the present oligotrophic conditions and to the oxygenation of deep layers, preventing denitrification and redox processes (Rogora et al., 2018). At the same time, Lake Maggiore is characterised by quite high NO_3 concentrations, mainly due to the nitrogen input from atmospheric deposition (Mosello et al., 2001).

Table 4 lists the final values of the phytoplankton parameters for the four functional groups. Specific tuning was performed for 31 out of 80 parameters. Unusually high growth rate and low standard, optimum and maximum temperatures were adopted for diatoms to reproduce their remarkably rapid, early and prominent blooms in cold waters and their early decay due to the spring bloom of zooplankton, not included in the model. Similar, less extreme parameters were employed for c3phytes, which bloom later in spring to much smaller biomasses. Very low phytoplankton temperature parameters were also used by Carraro et al. (2012) and Copetti et al. (2006) to reproduce very early blooms of similar phytoplankton assemblages in the neighbouring Lake Pusiano (Northern Italy). A respiration loss rate well outside the upper literature boundary was employed to model the late peak and low winter survival rate of dinophytes. The moderate winter concentrations of c3phytes were reproduced through a small value of the same parameter. Despite the approximation on nutrients wholly entering at the surface, adopted phosphorus parameters are all inside literature ranges, maximum internal P concentrations being set to the upper boundaries for diatoms and dinophytes. Peculiarly high internal nitrogen concentrations had to be used for the four functional groups to avoid excess NO_3 concentrations in the epilimnion, being spread to the hypolimnion with mixing events. These may be due to lacking nutrient immobilisation by heterotrophic bacteria, as well as possible input load overestimation.

3.2. Model results

The evaluations on water temperature modelling in Fenocchi et al. (2017) are still valid. The seasonal cycle of water temperature in the 0 ÷ 20 m layer is well reproduced (Fig. 4a), with comparable performances to literature (Table 5). An overestimation of summer epilimnetic temperatures is yet obtained in the 2007–2014 period, being maximum for 2013. A staircase-like evolution results in the 200 ÷ 370 m layer instead of the irregular observed trend (Fig. 4b). This should be ascribed to: 1) missing heat advection by deep intrusions of tributaries in the model; 2) approximate reproduction of deep mixing in all 1D models (Fenocchi et al., 2017, 2018); 3) absent local horizontal inhomogeneities, 1D models returning laterally averaged results; 4) analytical errors on observations. Goodness-of-fit metrics in the deep hypolimnion are nevertheless equivalent to published ones, with a particularly small $NMAE_m$ (Table 5). Homeothermic conditions correctly result at the end of winters 1999 and 2006 when complete-mixing events occurred.

The evolution of dissolved oxygen concentration in the 200 ÷ 370 m layer is well simulated (Fig. 5a), reproducing the replenishments from upper layers during full (1999, 2006) and partial (2000, 2004, 2005) turnovers. The simulated oxygen consumption curve in the validation period after the last chemical homogenisation is straighter than the observed one. Missing deep oxygen input from interflows and underestimated diffusion from water layers above would contribute to this mismatch. In addition, model parameters for O_2-consuming processes were calibrated over a period in which frequent deep mixing events occurred, whereas none of them occurred during validation. However, measured data for the last few years (2016–2018) agree with the steeper decrease of O_2 predicted by the model (Rogora et al., 2018). Optimal prediction of deep-water orthophosphate is obtained in calibration and validation (Fig. 5b), the accumulation curve being properly matched during the latter period. For nitrate (Fig. 5c), the model reproduces small concentration jumps in the deep hypolimnion with complete- and partial-mixing events, absent in the observations. This should be ascribed to a more heterogeneous modelled vertical distribution of NO_3 than the observed one. Observations also display a steadier nitrate concentration due to perfect equilibrium between nitrification and denitrification, which could not be fully reproduced. For deep-water O_2, PO_4 and NO_3, model performances are analogous or better than literature ones in calibration and validation (Table 5), with distinctly lower $NMAE_m$ values.

The model does not reproduce the short-scale irregularities of all chemical variables in the deep hypolimnion. Such issue is common to modelling studies (Burger et al., 2008; Copetti et al., 2006; Trolle et al., 2008a, 2008b, 2011) and should be credited to the same error sources identified for water temperature. High-frequency oscillations are particularly relevant for ammonium (Fig. 5d) and dissolved organic phosphorus (Fig. 5f) and nitrogen (Fig. 5g), their amplitude being comparable or predominant over that of inter-annual trends. This results in low, non-significant correlation coefficients and higher $NMAE_m$ values than for O_2, PO_4 and NO_3 (Table 5), even though inter-annual trends in the calibration and validation periods are visually satisfactorily reproduced. Comparing model results to moving averages of observed data for NH_4, DOP and DON in the deep hypolimnion leads to similar goodness-of-fit metrics to those of O_2, PO_4 and NO_3. For ammonium, the relevant observed oscillations should be mostly caused by the very low measured concentrations around or below the limit of detection (= 0.32 mmol N/m^3), producing an analytical error comparable to the actual signal (Cui et al., 2016; Gal et al., 2009; Li et al.,

Table 3
Adopted chemical parameters and literature ordinary ranges and outliers. Parameters that required specific tuning are indicated with *. Superscript letters refer to cited literature in Table 1, [AED] = Hipsey et al. (2013). References for adopted parameters are relative only to employed values in the cited studies, whereas for outliers they refer to both adopted values and given calibration/literature ranges.

Parameter	Description		Value	Range (Outliers)
Nitrogen				
Rnitrif [/d]	Maximum reaction rate of nitrification at 20 °C	*	0.34	0.01 ÷ 0.2 (0.005[f] ÷ 0.5[AED])
Rdenit [/d]	Maximum reaction rate of denitrification at 20 °C	*	0.000537	0.01 ÷ 0.1 (0.000864[q] ÷ 0.75[p])
Knitrif [mmol O_2/m^3]	Half-saturation oxygen concentration for nitrification		46.875[d]	46.875 ÷ 93.75 (15.625[h,q] ÷ 140.625[l])
Kdenit [mmol O_2/m^3]	Half-saturation oxygen concentration for denitrification		156.25[°]	12.5 ÷ 15.625 (6.25[l] ÷ 156.25[°])
theta_nitrif	Arrhenius temperature multiplier for nitrification		1.08[d,g,h,j,o,q,r,AED]	1.03 ÷ 1.08 (1.02[f] ÷ 1.14[f])
theta_denit	Arrhenius temperature multiplier for denitrification		1.08[g,h,o,q,r,AED]	1.045 ÷ 1.08
Organic matter: phosphorus				
w_pop [m/d]	Settling rate of POP		−1.0[AED]	−1.0 ÷ -0.1
Rpop_miner [/d]	Breakdown rate of POP at 20 °C	*	0.005	0.01 ÷ 0.03 (0.001[s] ÷ 0.5[AED])
Rdop_miner [/d]	Mineralisation rate of DOP at 20 °C	*	0.005	0.01 ÷ 0.05 (0.005[p] ÷ 0.5[AED])
Kpop_miner [mmol O_2/m^3]	Half-saturation oxygen concentration for POP breakdown		93.75[r]	46.875 ÷ 78.125 (31.25[AED] ÷ 156.25[g])
Kdop_miner [mmol O_2/m^3]	Half-saturation oxygen concentration for DOP mineralisation		93.75[r]	46.875 ÷ 78.125 (31.25[AED] ÷ 93.75[r])
theta_pop_miner	Arrhenius temperature multiplier for POP breakdown		1.08[g,AED]	1.02 ÷ 1.14 (1.18[h])
theta_dop_miner	Arrhenius temperature multiplier for DOP mineralisation		1.08[g,AED]	1.02 ÷ 1.14
Organic matter: nitrogen				
w_pon [m/d]	Settling rate of PON		−1.0[AED]	−1.0 ÷ -0.1
Rpon_miner [/d]	Breakdown rate of PON at 20 °C	*	0.011	0.005 ÷ 0.03 (0.003[g] ÷ 0.8[f])
Rdon_miner [/d]	Mineralisation rate of DON at 20 °C	*	0.011	0.003 ÷ 0.05 (0.00025[l] ÷ 0.8[f])
Kpon_miner [mmol O_2/m^3]	Half-saturation oxygen concentration for PON breakdown		156.25[g]	46.875 ÷ 78.125 (31.25[AED] ÷ 156.25[g])
Kdon_miner [mmol O_2/m^3]	Half-saturation oxygen concentration for DON mineralisation		156.25[g]	46.875 ÷ 78.125 (31.25[AED] ÷ 93.75[r])
theta_pon_miner	Arrhenius temperature multiplier for PON breakdown		1.08[g,AED]	1.02 ÷ 1.14 (1.18[h])
theta_don_miner	Arrhenius temperature multiplier for DON mineralisation		1.08[g,AED]	1.02 ÷ 1.14
Organic matter: carbon				
w_poc [m/d]	Settling rate of POC		−1.0[AED]	−1.0
Rpoc_miner [/d]	Breakdown rate of POC at 20 °C	*	0.001	0.001 ÷ 0.07 (0.5[AED])
Rdoc_miner [/d]	Mineralisation rate of DOC at 20 °C	*	0.001	0.001 ÷ 0.05 (0.5[AED])
Kpoc_miner [mmol O_2/m^3]	Half-saturation oxygen concentration for POC breakdown	*	156.25	46.875 ÷ 78.125 (31.25[AED] ÷ 93.75[r])
Kdoc_miner [mmol O_2/m^3]	Half-saturation oxygen concentration for DOC mineralisation	*	156.25	46.875 ÷ 78.125 (31.25[AED] ÷ 93.75[r])
theta_poc_miner	Arrhenius temperature multiplier for POC breakdown		1.08[g,AED]	1.02 ÷ 1.14 (1.18[h])
theta_doc_miner	Arrhenius temperature multiplier for DOC mineralisation		1.08[g,AED]	1.02 ÷ 1.14

2013; Trolle et al., 2011). Strong irregularities in the observed trends of DOP and DON would be also due to these being calculated variables, affected by analytical errors on both total and inorganic forms, in addition to oscillations of neglected POP and PON.

The worst agreement is attained for deep-water silica concentrations (Fig. 5e), for which an increase is correctly reproduced, yet with an improper staircase-like evolution. In addition to the error sources listed for water temperature, such behaviour is ascribable to the simplified silica cycle within AED2 (Hipsey et al., 2013).

Agreement of chemical variables in the 0 ÷ 20 m layer is less accurate. Straightforward causes are the chemical module being optimised in the deep hypolimnion and the assumption of all nutrients entering the lake at the surface. Most importantly, the annual cycles of nutrients in the epilimnion are much harder to reproduce than the long-term trends in deep waters, as surface values strongly depend on the quantitative accuracy of phytoplankton modelling. In addition, in oligotrophic systems as Lake Maggiore seasonal epilimnetic oscillations are not as clearly defined as in eutrophic ones, making model fit more difficult. Chemical variables are also more horizontally heterogeneous in the epilimnion, due to the higher interaction with physical and biological patchiness sources. Therefore, laboriously optimising chemical processes in the epilimnion could not produce a significant improvement. We herein report sample results for the limiting nutrient PO_4 (Fig. 6 and Table 5), whose annual cycle is adequately reproduced in the calibration period, with some underestimation. Model fit however degrades during validation together with that of phytoplankton, due to the strong influence of its uptake. Significant Pearson and Spearman correlation coefficients $R = 0.36$ and $R = 0.23$, $R_S = 0.39$ and $R_S = 0.29$ also result in the calibration period for epilimnetic NO_3 and NH_4, respectively.

For phytoplankton (Fig. 7; Table 5), cycling and succession among functional groups are satisfactorily reproduced, larger errors occurring in biomasses estimation, as also observed in Cui et al. (2016); Gal et al. (2009); Li et al. (2013); Özkundakci et al. (2011) and Rigosi et al. (2011). This is confirmed by the generally higher Spearman correlation coefficients than the Pearson ones in calibration and validation. The huge *Mougeotia* bloom in summer 2011 is not reproduced. As this distorts the validation error metrics for c3phytes and total Chl-*a*, values excluding 2011 are considered for such variables.

Pearson correlation coefficients for calibration and validation are higher than the average literature values for both total phytoplankton and individual groups. Equivalent to only slightly inferior performances are obtained for single functional groups compared to total Chl-*a* regarding annual cycling, as revealed by Spearman correlation coefficients. Worst correlations are obtained for the aggregated c3phytes group, due to the less specific calibrated parameters. Modelling of total Chl-*a* seems better than that of individual groups according to $NMAE_m$, whose values are all aligned with literature ones in calibration and validation, yet comparable performances result for $NMAE_r$.

Phytoplankton modelling deteriorates in validation. First, annual cycling is less accurate, as revealed by the decrease of Spearman correlation coefficients for total Chl-*a* and all functional groups except cyanophytes, being most relevant for diatoms. Second, a notable underestimation of peak concentrations occurs for cyanophytes and diatoms, whereas an overestimation is obtained for c3phytes, as highlighted by NME_m and NME_r. Underprediction results for total Chl-*a*, even if less evident than considering the total phytoplankton carbon concentration, highlighting the error of employing constant C:Chl-*a* ratios. Pearson correlation coefficients consequently decrease for all phytoplankton variables from calibration to validation, to a higher extent than Spearman ones. Accuracy variations between calibration and validation were not systematically observed in the considered literature studies, likely due to the short simulated periods (Table 1).

Table 4
Adopted phytoplankton parameters and literature ordinary ranges and outliers. Parameters which required specific tuning are indicated with *. Superscript letters refer to cited literature in Table 1, [AED] = Hipsey et al. (2013). References for adopted parameters are relative only to employed values in the cited studies, whereas for outliers they refer to both adopted values and given calibration/literature ranges.

Parameter	Description	Cyanophytes		Diatoms		Dinophytes		C3phytes	
		Value	Range (Outliers)	Value	Range (Outliers)	Value	Range (Outliers)	Value	Range (Outliers)
General									
w_p [m/d]	Settling rate (negative = sinking, positive = buoyant)	$0^{j,s}$	$-0.1 \div 0.43$ ($-50.37^{t} \div 3.11^{d}$)	$-0.86^{c,j,k,AED}$	$-0.86 \div -0.43$ ($-4924.8^{d} \div -0.05^{g}$)	$0^{h,j}$	0 ($-50.37^{t} \div 8.65^{t}$)	0	$-0.43 \div 0.43$ ($-50.37^{t} \div 0.87^{t}$)
Ycc [mg C/mg Chl-*a*]	C:Chl-*a* ratio	50^{d}	$40 \div 50$ ($27^{i} \div 150^{i}$)	* 50	40 (32^{i})	* 40	67^{i}	$40^{b,d,g,r}$	$30 \div 40$
Growth									
R_growth [/d]	Phytoplankton maximum growth rate at 20 °C *	2.9	$0.41 \div 2.1$ ($0.048^{d} \div 3.63^{a}$)	* 9.6	$1.0 \div 3.6$ ($0.2^{t} \div 4.0^{l}$)	* 2.4	$0.35 \div 1.5$ ($0.175^{l} \div 4.56^{h,j,k}$)	* 5.4	$0.2 \div 3.6$ ($0.12^{a} \div 8.57^{d}$)
theta_growth	Arrhenius temperature multiplier for growth	1.08^{*}	$1.04 \div 1.1$ ($1.02^{a} \div 1.14^{a,t}$)	$1.08^{d,j,k}$	$1.06 \div 1.11$ ($1.01^{b} \div 1.14^{t}$)	1.08	$1.06 \div 1.1$ (1.14^{t})	$1.08^{b,d,t}$	$1.06 \div 1.1$ ($1.02^{a} \div 1.14^{a,t}$)
T_std [°C]	Standard temperature	$20^{g,o,u,AED}$	$19 \div 24$ ($10^{a,b}$)	* 7	$13 \div 20$ (8^{b})	20^{h}	$19 \div 20$	* 7	20 (15^{b})
T_opt [°C]	Optimum temperature	24^{e}	$20 \div 30$ ($13^{b} \div 34^{d}$)	* 12	$16 \div 25$ (12^{b})	* 22	$22 \div 24$	* 14	$21 \div 28$ ($14^{d} \div 32^{a}$)
T_max [°C]	Maximum temperature	$35^{e,j,k,o,u,AED}$	$34 \div 40$ (20^{b})	* 18	$22 \div 27$ ($21^{e} \div 33^{b}$)	30^{h}	$28 \div 32$	* 21	$33 \div 35$ ($25^{b} \div 40^{a}$)
Light									
I_K [μE/(m^2 s)]	Half-saturation constant for light limitation of growth	$130^{g,AED}$	$120 \div 150$ ($75^{l} \div 225^{l}$)	50^{c}	$35 \div 60$ (10^{n})	40^{n}	40	$100^{a,g}$	$20 \div 100$ (300^{a})
Respiration									
f_pr	Fraction of primary production lost to exudation	$0.014^{d,g,j,k}$	0.014	$0.014^{d,g,j,k}$	0.014	$0.014^{j,k}$	0.014	$0.014^{d,g}$	0.014 (0.01^{r})
R_resp [/d]	Respiration/metabolic loss rate at 20 °C *	0.083	$0.015 \div 0.118$ ($0.001^{a} \div 0.177^{l}$)	* 0.084	$0.05 \div 0.085$ ($0.01^{d,h} \div 0.3^{b}$)	* 0.162	$0.03 \div 0.08$ (0.02^{h})	* 0.047	$0.05 \div 0.135$ ($0.001^{a} \div 0.18^{b}$)
theta_resp	Arrhenius temperature multiplier for respiration	1.08	$1.04 \div 1.1$ ($1.02^{a} \div 1.14^{a,e}$)	1.08^{d}	$1.05 \div 1.12$	1.08	$1.05 \div 1.06$ (1.1^{t})	1.08^{r}	$1.05 \div 1.1$ ($1.02^{a} \div 1.14^{a}$)
k_fres	Fraction of metabolic loss that is true respiration	$0.25^{j,k,AED}$	0.25 (0.8^{d})	$0.25^{j,k,AED}$	0.25 (0.5^{d})	$0.25^{j,k}$	0.25 (0.4^{h})	0.25^{AED}	$0.25 \div 0.3$ (0.8^{d})
k_fdom	Fraction of metabolic loss that is DOM	$0.2^{j,k,AED}$	0.2 ($0.1^{d} \div 0.3^{d}$)	$0.05^{j,k}$	$0.05 \div 0.2$ (0.5^{d})	$0.2^{j,k}$	0.2 (0.1^{h})	0.2^{AED}	$0.1 \div 0.2$
Phosphorus									
K_P [mmol P/m^3]	Half-saturation concentration of P	0.26^{g}	$0.04 \div 0.32$ ($0.01^{t} \div 1.29^{t}$)	$0.23^{c,g}$	$0.09 \div 0.36$ ($0.003^{t} \div 1.29^{t}$)	$0.08^{j,k}$	$0.03 \div 0.15$ ($0.003^{t} \div 1.29^{t}$)	* 0.20	$0.06 \div 0.81$ ($0.003^{t} \div 1.29^{t}$)
X_pmin [mmol P/mmol C]	Minimum internal P concentration *	0.004	$0.002 \div 0.006$ ($0.001^{d} \div 0.009^{l}$)	* 0.004	$0.003 \div 0.005$ ($0.002^{l} \div 0.008^{d}$)	* 0.004	$0.002 \div 0.002$ ($0.0001^{j,k,l}$)	* 0.004	$0.002 \div 0.008$
X_pmax [mmol P/mmol C]	Maximum internal P concentration	0.009^{d}	$0.009 \div 0.504$	$0.033^{d,h}$	$0.023 \div 0.033$ ($0.006^{n} \div 0.035^{l}$)	$0.007^{h,n}$	$0.001 \div 0.007$	0.023^{d}	$0.023 \div 0.023$
R_puptake [mmol P/(m^3 d)]	Maximum P uptake rate *	0.006	$0.031 \div 0.097$ ($0.004^{d} \div 0.145^{l}$)	* 0.007	$0.001 \div 0.007$ (0.23^{l})	* 0.006	$0.001 \div 0.004$ ($0.0002^{h,j,k}$)	* 0.005	0.003
Nitrogen									
K_N [mmol N/m^3]	Half-saturation concentration of N	$2.14^{g,o}$	$1.43 \div 5.78$ ($0.07^{d,j,k} \div 14.28^{t}$)	$4.28^{d,g}$	$3.57 \div 4.28$ ($0.43^{p} \div 14.28^{t}$)	$7.14^{j,k}$	$7.14 \div 8.64$ ($1.36^{m} \div 27.13^{h,j,k}$)	$2.14^{d,s}$	$1.43 \div 4.28$ ($0.71^{p} \div 14.28^{t}$)
X_ncon [mmol N/mmol C]	Constant internal N concentration *	0.38	$0.05 \div 0.2$ (0.21^{d})	* 0.52	$0.13 \div 0.19$ (0.06^{l})	* 0.77	$0.06 \div 0.09$ (0.03^{l})	* 0.83	$0.12 \div 0.19$
Silica									
K_Si [mmol Si/m^3]	Half-saturation concentration of Si	–	–	1.0^{c}	$1.0 \div 2.99$ (8.55^{b})	–	–	1.0	–
X_sicon [mmol Si/mmol C]	Constant internal Si concentration	–	–	0.4^{AED}	–	–	–	* 0.1	–

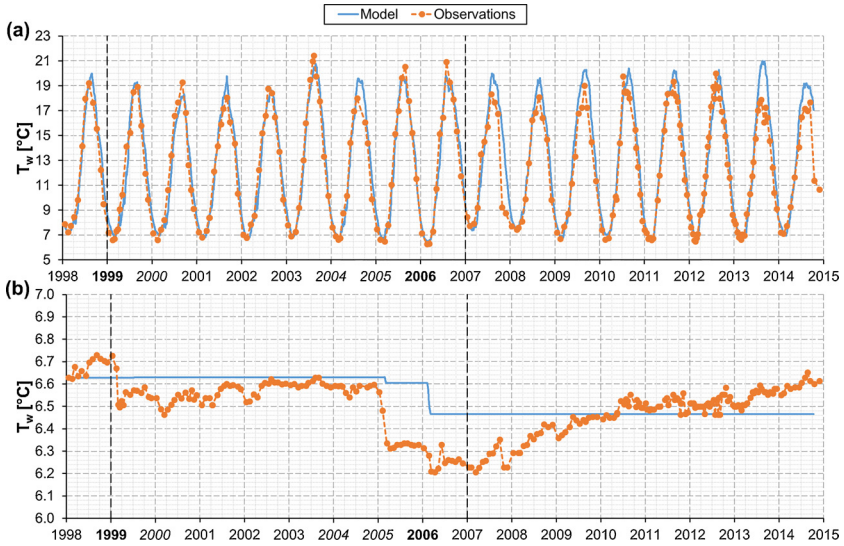

Fig. 4. Modelled and observed water temperatures in the 0 ÷ 20 m (a) and 200 ÷ 370 m (b) layers. Years with full and partial turnovers are marked in bold and italics, respectively. Model spin-up, calibration and validation periods are separated by dashed lines.

3.3. Model validity

The performances of the present coupled ecological-hydrodynamic model of Lake Maggiore in calibration and validation are equivalent, if not superior, to those of literature studies (Table 5) for shallower and smaller lakes over shorter periods (Table 1). The chemical evolution of the deep hypolimnion throughout the simulated period is well reproduced, especially for dissolved oxygen and orthophosphate (Fig. 5, Table 5), whose future trends are of great concern in relation to climate change. Lake Maggiore, as the other deep lakes south of the Alps, is already showing a decrease of O_2 and an accumulation of PO_4 in deep waters (Rogora et al., 2018; see also Figs. 5a-5b), due to the increasing water column stability brought by climate warming (Fenocchi et al., 2018). The much smaller $NMAE_m$ values obtained for deep-water chemical variables compared to literature studies (Table 5) descend also from the great depth of Lake Maggiore, whose deep hypolimnion is isolated from seasonal primary production, so that its modelling is mostly unaffected by errors on phytoplankton. Reproduction of phytoplankton is satisfactory even for single functional groups, yet model performances decrease during validation (Fig. 7; Table 5). This is due to the extensive parameterisation of biological processes and the consequent dependence on calibration.

Shifts in the assemblages of functional groups are a fundamental source of error in phytoplankton modelling and cannot be reproduced unless all individual species entered the model, leading to a prohibitive number of parameters. During the calibration period, substantial stability of the dominant species established with oligotrophication in the early 1990s was observed in Lake Maggiore (CNR-ISE, 2003, 2008; Morabito et al., 2012), likely allowing suitable calibration results to be attained. Yet, some obtained discrepancies in that period should still be ascribed to inter-annual changes in the proportions among species and in the physiology of the same species with adaptation. Compositional shifts of diatoms and cyanophytes towards species typical of more nutrient-enriched waters, which had been dominant during eutrophication, were observed in the validation period (CNR-ISE, 2013, 2016; Marchetto et al., 2004). Such changes would explain the performance drop in validation for these two groups (Figs. 7b-7c; Table 5). The overestimation of summer epilimnetic temperatures in the validation period (Fig. 4a; Table 5) may contribute to the underestimation of diatoms. The missing exceptional *Mougeotia* bloom in 2011 (Fig. 7e) is unavoidable, since a specific functional group for the taxon would have been needed, its parameterisation yet eluding the present knowledge as the positive conditions for growth are not clear (Tapolczai et al., 2015).

Recent changes in phytoplankton assemblages in Lake Maggiore occurred despite stable nutrient loads (Fig. 2) and oligotrophic conditions according to total Chl-*a* (Fig. 7a). These shifts could have been triggered by the shallower mixing depths and the surface warming (Fig. 4a) occurred after 2006, the new dominant species favouring warmer and more stratified waters (CNR-ISE, 2016). Even if physical factors, which are the main drivers of phytoplankton evolution under nutrient limitation (Morabito et al., 2012), are simulated by the coupled model, the inability to reproduce species shifts would be a severe limitation when forecasting climate change effects, as blooms of new dominant species would not be detected (Bruce et al., 2006; Özkundakci et al., 2011; Snortheim et al., 2017). Phytoplankton shifts would increase in the future, as surface water temperature and lake stratification are set to keep increasing (Fenocchi et al., 2018; Salmaso, 2010). Adopting multiple functional groups, as done here, would hence allow better long-term results than using a single variable, as some large-scale features of phytoplankton shifting could be reproduced. Future shifts in phytoplankton species could also be caused by shifts at higher ecosystem levels, not even explicitly modelled herein, through different predation, as happened in the past for Lake Maggiore (Manca and Ruggiu, 1998).

Latest phytoplankton blooms under oligotrophic conditions have been speculated to be supported by scarcely detectable nutrient inputs such as diffuse sources during impulse rainfalls (Callieri et al., 2014; Morabito et al., 2018). Such feeding is not included in the present model, in which diffuse runoff and groundwater input are neglected and mean monthly discharges and isolated sampled concentrations at the main tributaries were employed to calculate input loads. Approximate nutrient loads also contribute to general discrepancies on chemical and biological variables. Errors in the estimation of missing discharges should also be considered. In addition, the approximate monthly frequency of water chemistry and phytoplankton observations used for model calibration and validation is probably too sparse to catch epilimnetic seasonal variability. Discrepancies coming from input loads all entering at the surface should finally be recognised.

Horizontal heterogeneity is another fundamental error source. Patchiness peaks at the surface due to maximum influence of non-uniform external factors and declines with depth due to growing isolation and inertia. The validity of the 1D hypothesis therefore increases with depth, though some patchiness still affects chemical variables in the deep hypolimnion due to non-uniform mixing at small spatial and time scales. Phytoplankton patchiness is most relevant, depending on the combination of horizontal physical, chemical and biological

Table 5
Goodness-of-fit metrics for water temperature, chemical and phytoplankton variables in the calibration and validation periods. For correlation coefficients: *: $p < 0.001$, †: $0.001 \leq p < 0.01$, ‡: $0.01 \leq p < 0.05$, §: $p \geq 0.05$. Validation indices including 2011 are given in parentheses for c3phytes and total Chl-*a*. Means and standard deviations of literature metrics are provided for *R* and $NMAE_m$, with sample sizes in square brackets. Samples include values for both calibration and validation. Epilimnion or surface metrics and hypolimnion or bottom metrics were respectively considered for 0 ÷ 20 m and 200 ÷ 370 m variables when available.

Variable	R			R_S		$NMAE_m$			$NMAE_r$		NME_m		NME_r	
	Cal.	Val.	Lit.	Cal.	Val.	Cal.	Val.	Lit.	Cal.	Val.	Cal.	Val.	Cal.	Val.
T_w (0 ÷ 20 m)	0.98*	0.97*	0.98 ± 0.02 [21]	0.98*	0.96*	6%	8%	7% ± 4% [12]	6%	9%	1%	6%	1%	6%
T_w (200 ÷ 370 m)	0.81*	0.84*	0.88 ± 0.12 [21]	0.73*	0.73*	2%	1%	10% ± 5% [12]	–	–	2%	0%	–	–
O_2 (200 ÷ 370 m)	0.83*	0.79*	0.88 ± 0.05 [22]	0.84*	0.76*	5%	7%	19% ± 10% [16]	–	–	0%	4%	–	–
PO_4 (200 ÷ 370 m)	0.61*	0.70*	0.60 ± 0.26 [22]	0.61*	0.73*	19%	12%	78% ± 27% [14]	–	–	−1%	3%	–	–
NO_3 (200 ÷ 370 m)	0.69*	0.83*	0.56 ± 0.33 [19]	0.77*	0.84*	4%	2%	68% ± 26% [14]	–	–	2%	−1%	–	–
NH_4 (200 ÷ 370 m)	0.31†	−0.19§	0.58 ± 0.28 [21]	0.31†	−0.11§	45%	51%	76% ± 31% [16]	–	–	1%	−26%	–	–
SiO_2 (200 ÷ 370 m)	0.13§	0.00§	0.82 ± 0.01 [2]	−0.16§	0.00§	14%	3%	52% ± 4% [2]	–	–	−5%	1%	–	–
DOP (200 ÷ 370 m)	0.15§	−0.17§	–	0.13§	−0.22‡	45%	57%	–	–	–	−2%	−49%	–	–
DON (200 ÷ 370 m)	0.12§	−0.15§	–	0.12§	−0.03§	36%	50%	–	–	–	−2%	−40%	–	–
PO_4 (0 ÷ 20 m)	0.69*	0.27†	0.52 ± 0.29 [22]	0.57*	0.14	49%	62%	82% ± 28% [14]	24%	49%	−37%	−59%	−18%	−47%
Total Chl-*a* (0 ÷ 20 m)	0.69*	0.41* (0.19§)	0.36 ± 0.26 [20]	0.65*	0.53* (0.51*)	38%	39% (44%)	56% ± 24% [11]	22%	24% (22%)	−1%	−12% (-21%)	−1%	−8% (-11%)
Cyanophytes (0 ÷ 20 m)	0.65*	0.44*	0.50 ± 0.29 [5]	0.67*	0.70*	69%	72%	69% ± 26% [4]	22%	21%	−3%	−51%	−1%	−15%
Diatoms (0 ÷ 20 m)	0.70*	0.40*	0.29 ± 0.19 [5]	0.66*	0.37*	63%	78%	85% ± 34% [5]	18%	21%	−3%	−54%	−1%	−14%
Dinophytes (0 ÷ 20 m)	0.59*	0.48*	0.30 ± 0.01 [3]	0.69*	0.65*	72%	76%	64% ± 26% [3]	20%	20%	−1%	−2%	0%	0%
C3phytes (0 ÷ 20 m)	0.49*	0.37* (−0.08§)	–	0.39*	0.33† (0.21‡)	58%	85% (94%)	–	25%	39% (15%)	−3%	33% (-62%)	−1%	15% (-10%)

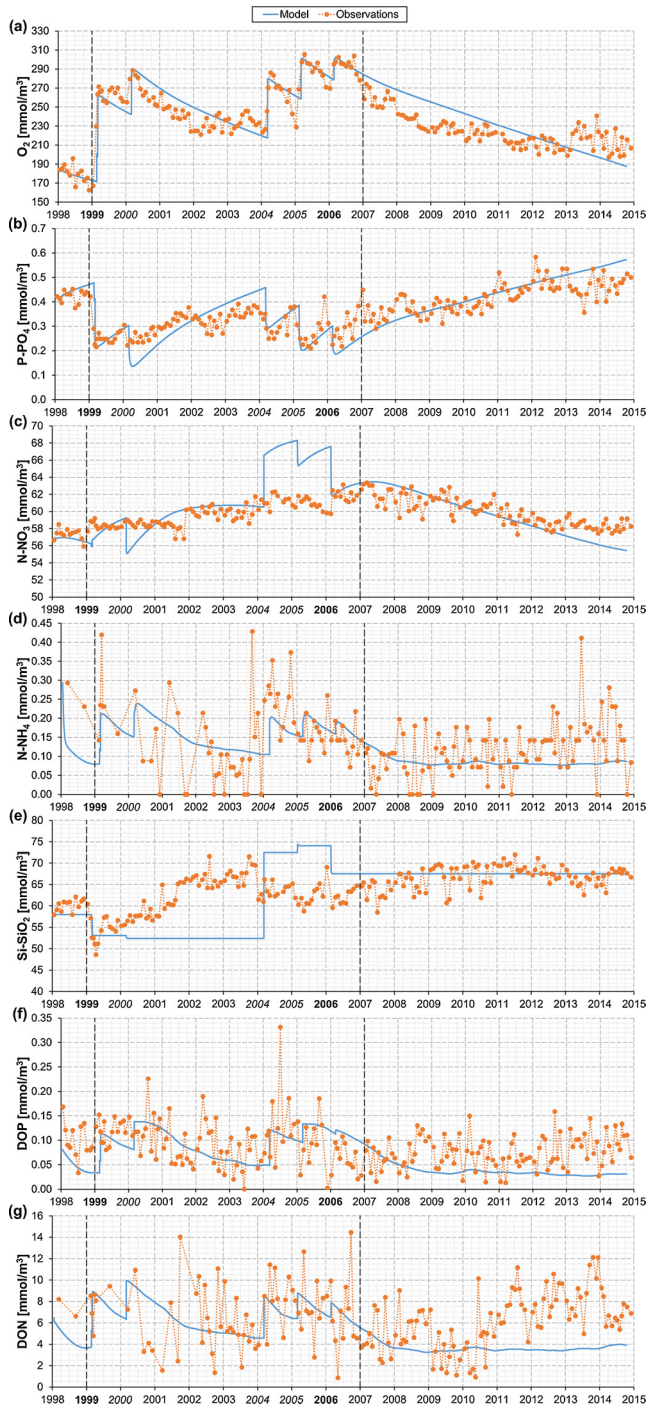

Fig. 5. Modelled and observed concentrations of O_2 (a), PO_4 (b), NO_3 (c), NH_4 (d), SiO_2 (e), DOP (f) and DON (g) in the 200 ÷ 370 m layer. Years with full and partial turnovers are marked in bold and italics, respectively. Model spin-up, calibration and validation periods are separated by dashed lines.

heterogeneities (Hillmer et al., 2008; Kara et al., 2012). Systematic horizontal heterogeneity patterns observed in the vertical samples over longer time scales are included into the calibrated parameters, causing a drop of performances if they change during validation (Hillmer et al., 2008), an issue which we cannot exclude for the present case. Theoretically, a 1D model could return results that better describe laterally averaged conditions than those in the vertical samples. In this regard, the Ghiffa station is in the centre of Lake Maggiore and has been demonstrated to experience average surface water temperature, epilimnion thickness, chemical and phytoplankton trends to those of the

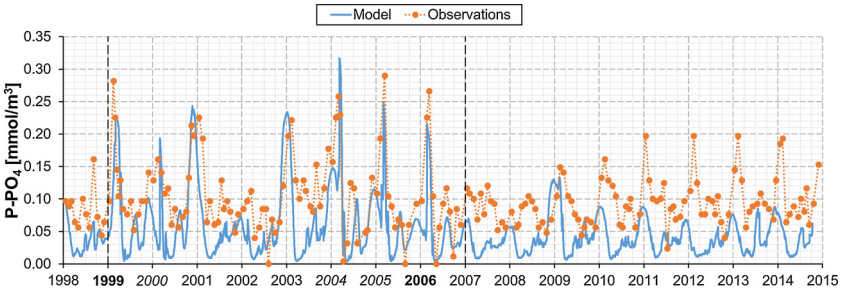

Fig. 6. Modelled and observed concentrations of PO_4 in the 0 ÷ 20 m layer. Years with full and partial turnovers are marked in bold and italics, respectively. Model spin-up, calibration and validation periods are separated by dashed lines.

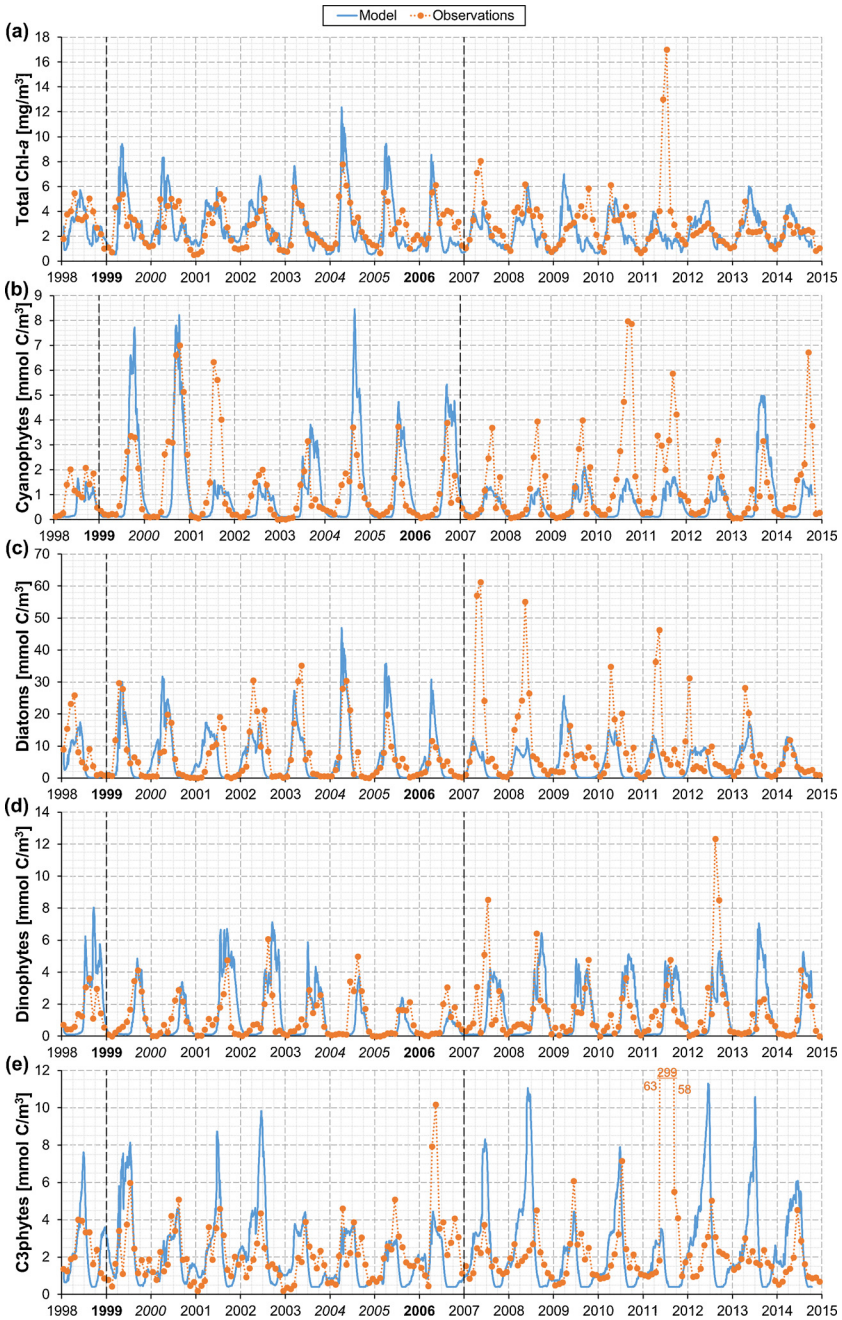

Fig. 7. Modelled and observed total Chl-*a* concentrations (a) and carbon concentrations of cyanophytes (b), diatoms (c), dinophytes (d) and c3phytes (e) in the 0 ÷ 20 m layer. Years with full and partial turnovers are marked in bold and italics, respectively. Model spin-up, calibration and validation periods are separated by dashed lines.

northern and southern regions (CNR-ISE, 2013b). The casual patchiness at local and brief time scales instead cannot be represented by 1D models and represents a significant part of the error due to phytoplankton horizontal heterogeneity in the present case.

Given the limits discussed above, a modelling application targeting phytoplankton succession alone, specialising chemical variables calibration in the epilimnion, could not give much better results than the present ones. In fact, a less parametrical ecosystem description would be needed to significantly improve the forecasting performances under changing conditions (Schladow and Hamilton, 1997). Progress in the description of biochemical processes could make models less dependent on calibration and hence on data availability. Otherwise, observation availability would keep impairing coupled ecological-hydrodynamic modelling. In this study, we were able to calibrate the model over an extended period and accomplish a thorough analysis of results thanks to the large dataset available for Lake Maggiore. Yet, we still had to adopt some simplifications due to the lack of information, which increased the dependence on parameterisation, thus impacting model performances in validation.

4. Conclusions

The present application of GLM-AED2 to Lake Maggiore over 1998–2014 has shown that, through extensive calibration, 1D coupled ecological-hydrodynamic models can have for prolonged simulations of deep large lakes comparable performances to those found in literature for shallower and smaller lakes over shorter periods. The chemical evolution of the deep hypolimnion was successfully reproduced, also thanks to proper simulation of mixing dynamics. A noteworthy decrease of model performances was yet detected in validation for phytoplankton and epilimnetic water chemistry, due to the dependence on parameterisation.

The duration and peculiar features of the considered calibration and validation periods highlighted some relevant limits of coupled models for long-term prognoses of climate change effects on phytoplankton, especially for basins with stable oligotrophic loading and reduced mixing, as expected for many oligomictic lakes in the Western world for the 21st century. The impossibility to reproduce shifts in phytoplankton species stands out against other factors. Nevertheless, the forecasting abilities would be compatible with management purposes, the feedback to nutrient load variations over single years being qualitatively reproduced. Features such as variations in the timing of the succession and in the proportions among functional groups could also be inferred. A single application can address hypolimnetic chemistry and phytoplankton evolution in deep temperate lakes, given the marginal benefits of specific models. Quantitative results should be interpreted with care, according to the limitations and assumptions behind each model. Experience from validation may help to characterise the forecasting behaviour of a model, yet unexpected errors may always arise with changing external conditions. These may especially originate from out-of-bounds parameter values employed to amend for improperly described biochemical processes, which could potentially cause relevant non-linear misbehaviours. Comparison against a reference scenario without variations in climate and nutrient loads is strongly recommended to critically frame the obtained results.

Acknowledgments and Data

The limnological and meteorological data used in the present study were collected through the research programs funded for Lake Maggiore by the International Commission for the Protection of Italian-Swiss Waters (CIPAIS). We thank the technical and scientific staff of CNR-IRSA in Verbania Pallanza involved in the field work and data analyses and management through the years. Data for the Verbania Pallanza weather station from 2009 onwards were supplied by the Regional Environmental Protection Agency of Piedmont (ARPA Piemonte). Data for the Locarno-Monti weather station were provided by MeteoSwiss. Discharges for Rivers Maggia and Verzasca were obtained from the Swiss Federal Office for the Environment (UFAM). Limnological research on Lake Maggiore is performed within the framework of the LTER (Long-Term Ecological Research) Italian and European networks (site “Southern Alpine Lakes”, LTER_EU_IT_008).

We are deeply grateful to Giuseppe Morabito for contributing despite his precarious health. Even after his passing, the insightful comments that he had left over the years largely helped us to discuss the present results. He will be greatly missed.

References

Alewell, C., Manderscheid, B., 1998. Use of objective criteria for the assessment of biogeochemical ecosystem models. Ecol. Model. 107 (2-3), 213–224. https://doi.org/10.1016/S0304-3800(97)00218-4.

Ambrosetti, W., Barbanti, L., 1999. Deep water warming in lakes: an indicator of climatic change. J. Limnol. 58 (1), 1–9. https://doi.org/10.4081/jlimnol.1999.1.

Bertoni, R., Callieri, C., 1992. Organic carbon trend during the oligotrophication of Lago Maggiore. Memorie dell’Istituto Italiano di Idrobiologia 52, 191–205.

Bruce, L.C., Hamilton, D., Imberger, J., Gal, G., Gophen, M., Zohary, T., Hambright, K.D., 2006. A numerical simulation of the role of zooplankton in C, N and P cycling in Lake Kinneret. Israel. Ecol. Model. 193 (3-4), 412–436. https://doi.org/10.1016/j.ecolmodel.2005.09.008.

Bruce, L.C., Jellison, R., Imberger, J., Melack, J.M., 2008. Effect of benthic boundary layer transport on the productivity of Mono Lake. California. Saline Systems 4 (11). https://doi.org/10.1186/1746-1448-4-11.

Burger, D.F., Hamilton, D.P., Pilditch, C.A., 2008. Modelling the relative importance of internal and external nutrient loads on water column nutrient concentrations and phytoplankton biomass in a shallow polymictic lake. Ecol. Model. 211 (3-4), 411–423. https://doi.org/10.1016/j.ecolmodel.2007.09.028.

Callieri, C., Bertoni, R., Contesini, M., Bertoni, F., 2014. Lake level fluctuations boost toxic cyanobacterial “oligotrophic blooms”. PLoS One 9 (10), e109526. https://doi.org/10.1371/journal.pone.0109526.

Carraro, E., Guyennon, N., Hamilton, D., Valsecchi, L., Manfredi, E.C., Viviano, G., Salerno, F., Tartari, G., Copetti, D., 2012. Coupling high-resolution measurements to a three-dimensional lake model to assess the spatial and temporal dynamics of the cyanobacterium *Planktothrix rubescens* in a medium-sized lake. Hydrobiologia 698 (1), 77–95. https://doi.org/10.1007/s10750-012-1096-y.

CNR-ISE (CNR–Istituto per lo Studio degli Ecosistemi), 2003. Studies on the Evolution of Lake Maggiore: Limnological Aspects (*Ricerche Sull’evoluzione Del Lago Maggiore: Aspetti Limnologici*). Five-year Program 1998-2002, 2002 Campaign and Five-year Report. CIPAIS (*Commissione Internazionale per la Protezione delle Acque Italo-Svizzere*), Verbania Pallanza, Italy *in Italian*. http://www.cipais.org.

CNR-ISE (CNR – Istituto per lo Studio degli Ecosistemi), 2013. Studies on the Evolution of Lake Maggiore: Limnological Aspects (*Ricerche Sull’evoluzione Del Lago Maggiore: Aspetti Limnologici*). Five-year Program 2008-2012, 2012 Campaign and Five-year Report. CIPAIS (*Commissione Internazionale per la Protezione delle Acque Italo-Svizzere*), Verbania Pallanza, Italy *in Italian*. http://www.cipais.org.

CNR-ISE (CNR – Istituto per lo Studio degli Ecosistemi), 2008. Studies on the Evolution of Lake Maggiore: Limnological Aspects (*Ricerche Sull’evoluzione Del Lago Maggiore: Aspetti Limnologici*). Five-year Program 2003-2007, 2007 Campaign and Five-year Report. CIPAIS (*Commissione Internazionale per la Protezione delle Acque Italo-Svizzere*), Verbania Pallanza, Italy *in Italian*. http://www.cipais.org.

CNR-ISE (CNR – Istituto per lo Studio degli Ecosistemi), 2016. Studies on the Evolution of Lake Maggiore: Limnological Aspects (*Ricerche Sull’evoluzione Del Lago Maggiore: Aspetti Limnologici*). Three-year Program 2013-2015, 2015 Campaign and Three-year Report. CIPAIS (*Commissione Internazionale per la Protezione delle Acque Italo-Svizzere*), Verbania Pallanza, Italy *in Italian*. http://www.cipais.org.

Copetti, D., Tartari, G., Morabito, G., Oggioni, A., Legnani, E., Imberger, J., 2006. A biogeochemical model of Lake Pusiano (North Italy) and its use in the predictability of phytoplankton blooms: first preliminary results. J. Limnol. 65 (1), 59–64. https://doi.org/10.4081/jlimnol.2006.59.

Cui, Y., Zhu, G., Li, H., Luo, L., Cheng, X., Jin, Y., Trolle, D., 2016. Modeling the response of phytoplankton to reduced external nutrient load in a subtropical Chinese reservoir using DYRESM-CAEDYM. Lake Reserv. Manage. 32 (2), 146–157. https://doi.org/10.1080/10402381.2015.1136365.

Dietzel, A., Mieleitner, J., Kardaetz, S., Reichert, P., 2013. Effects of changes in the driving forces on water quality and plankton dynamics in three Swiss lakes – long-term simulations with BELAMO. Freshwater Biol. 58 (1), 10–35. https://doi.org/10.1111/fwb.12031.

Fenocchi, A., Rogora, M., Sibilla, S., Dresti, C., 2017. Relevance of inflows on the thermodynamic structure and on the modeling of a deep subalpine lake (Lake Maggiore, Northern Italy/Southern Switzerland). Limnologica 63, 42–56. https://doi.org/10.1016/j.limno.2017.01.006.

Fenocchi, A., Rogora, M., Sibilla, S., Ciampittiello, M., Dresti, C., 2018. Forecasting the evolution in the mixing regime of a deep subalpine lake under climate change scenarios through numerical modelling (Lake Maggiore, Northern Italy/Southern Switzerland). Clim. Dynam. 51 (9-10), 3521–3536. https://doi.org/10.1007/s00382-018-4094-6.

Gal, G., Hipsey, M.R., Parparov, A., Wagner, U., Makler, V., Zohary, T., 2009. Implementation of ecological modeling as an effective management and investigation

tool: Lake Kinneret as a case study. Ecol. Model. 220 (13-14), 1697–1718. https://doi.org/10.1016/j.ecolmodel.2009.04.010.
Gal, G., Makler-Pick, V., Shachar, N., 2014. Dealing with uncertainty in ecosystem model scenarios: application of the single-model ensemble approach. Environ. Model. Softw. 61, 360–370. https://doi.org/10.1016/j.envsoft.2014.05.015.
Grzybowski, M., 2014. Natural dimictic and polymictic lakes: similarities and differences in relationships among chlorophyll, nutrients, Secchi depth, and aquatic macrophytes. J. Freshwater Ecol. 29 (1), 53–69. https://doi.org/10.1080/02705060.2013.820153.
Guilizzoni, P., Galanti, G., Muntau, H., 1989. The aquatic macrophytes of Lake Maggiore: species composition, spatial distribution and heavy metal concentrations in tissue. Memorie dell'Istituto Italiano di Idrobiologia 46, 235–260.
Hamilton, D.P., Schladow, S.G., 1997. Prediction of water quality in lakes and reservoirs. Part I — model description. Ecol. Model. 96 (1-3), 91–110. https://doi.org/10.1016/S0304-3800(96)00062-2.
Hillmer, I., van Reenen, P., Imberger, J., Zohary, T., 2008. Phytoplankton patchiness and their role in the modelled productivity of a large, seasonally stratified lake. Ecol. Model. 218 (1-2), 49–59. https://doi.org/10.1016/j.ecolmodel.2008.06.017.
Hipsey, M.R., Bruce, L.C., Hamilton, D.P., 2013. Aquatic EcoDynamics (AED) model library: science manual. AED Report. The University of Western Australia, Perth, Australia.
Hipsey, M.R., Bruce, L.C., Hamilton, D.P., 2014. GLM - General Lake Model: model overview and user information. AED Report #26. The University of Western Australia, Perth, Australia.
Jöhnk, K.D., Huisman, J., Sharples, J., Sommeijer, B., Visser, P.M., Stroom, J.M., 2008. Summer heatwaves promote blooms of harmful cyanobacteria. Glob. Change Biol. 14 (3), 495–512. https://doi.org/10.1111/j.1365-2486.2007.01510.x.
Jørgensen, S.E., 1999. State-of-the-art of ecological modelling with emphasis on development of structural dynamic models. Ecol. Model. 120 (2-3), 75–96. https://doi.org/10.1016/S0304-3800(99)00093-9.
Kamenir, Y., Morabito, G., 2009. Lago Maggiore oligotrophication as seen from the long-term evolution of its phytoplankton taxonomic size structure. J. Limnol. 68 (1), 146–161. https://doi.org/10.4081/jlimnol.2009.146.
Kara, E.M., Hanson, P., Hamilton, D., et al., 2012. Time-scale dependence in numerical simulations: assessment of physical, chemical, and biological predictions in a stratified lake at temporal scales of hours to months. Environ. Model. Softw. 35, 104–121. https://doi.org/10.1016/j.envsoft.2012.02.014.
Kerimoglu, O., Jacquet, S., Vinçon-Leite, B., Lemaire, B.J., Rimet, F., Soulignac, F., Trévisan, D., Anneville, O., 2017. Modelling the plankton groups of the deep, perialpine Lake Bourget. Ecol. Model. 359, 415–433. https://doi.org/10.1016/j.ecolmodel.2017.06.005.
Li, Y., Waite, A.M., Gal, G., Hipsey, M.R., 2013. An analysis of the relationship between phytoplankton internal stoichiometry and water column N:P ratios in a dynamic lake environment. Ecol. Model. 252, 196–213. https://doi.org/10.1016/j.ecolmodel.2012.06.021.
Manca, M., Ruggiu, D., 1998. Consequences of pelagic food-web changes during a long-term lake oligotrophication process. Limnol. Oceanogr. 43 (6), 1368–1373. https://doi.org/10.4319/lo.1998.43.6.1368.
Marcé, R., Moreno-Ostos, E., García-Barcina, J.M., Armengol, J., 2010. Tailoring dam structures to water quality predictions in new reservoir projects: assisting decision-making using numerical modeling. J. Environ. Manage. 91 (6), 1255–1267. https://doi.org/10.1016/j.jenvman.2010.01.014.
Marchetto, A., Lami, A., Musazzi, S., Massaferro, J., Langone, L., Guilizzoni, P., 2004. Lake Maggiore (N. Italy) trophic history: fossil diatom, plant pigments, and chironomids, and comparison with long-term limnological data. Quat. Int. 113 (1), 97–110. https://doi.org/10.1016/S1040-6182(03)00082-X.
Martins, G., Ribeiro, D.C., Pacheco, D., Cruz, J.V., Cunha, R., Gonçalves, V., Nogueira, R., Brito, A.G., 2008. Prospective scenarios for water quality and ecological status in Lake Sete Cidades (Portugal): The integration of mathematical modelling in decision processes. Appl. Geochem. 23 (8), 2171–2181. https://doi.org/10.1016/j.apgeochem.2008.03.001.
Mieleitner, J., Borsuk, M., Bürgi, H.-R., Reichert, P., 2008. Identifying functional groups of phytoplankton using data from three lakes of different trophic state. Aquat. Sci. 70 (1), 30–46. https://doi.org/10.1007/s00027-007-0940-z.
Mieleitner, J., Reichert, P., 2008. Modelling functional groups of phytoplankton in three lakes of different trophic state. Ecol. Model. 211 (3-4), 279–291. https://doi.org/10.1016/j.ecolmodel.2007.09.010.
Morabito, G., Oggioni, A., Austoni, M., 2012. Resource ratio and human impact: how diatom assemblages in Lake Maggiore responded to oligotrophication and climatic variability. Hydrobiologia 698 (1), 47–60. https://doi.org/10.1007/s10750-012-1094-0.
Morabito, G., Rogora, M., Austoni, M., Ciampittiello, M., 2018. Could the extreme meteorological events in Lake Maggiore watershed determine a climate-driven eutrophication process? Hydrobiologia 824 (1), 163–175. https://doi.org/10.1007/s10750-018-3549-4.
Mosello, R., Barbieri, A., Brizzio, M.C., Calderoni, A., Marchetto, A., Passera, S., Rogora, M., Tartari, G., 2001. Nitrogen budget of Lago Maggiore: the relative importance of atmospheric deposition and catchment sources. J. Limnol. 60 (1), 27–40. https://doi.org/10.4081/jlimnol.2001.27.
Omlin, M., Reichert, P., Forster, R., 2001. Biogeochemical model of Lake Zürich: model equations and results. Ecol. Model. 141 (1-3), 77–103. https://doi.org/10.1016/S0304-3800(01)00256-3.
Özkundakci, D., Hamilton, D.P., Trolle, D., 2011. Modelling the response of a highly eutrophic lake to reductions in external and internal nutrient loading. N. Z. J. Mar. Freshwater Res. 45 (2), 165–185. https://doi.org/10.1080/00288330.2010.548072.
Pareeth, S., Bresciani, M., Buzzi, F., Leoni, B., Lepori, F., Ludovisi, A., Morabito, G., Adrian, R., Neteler, M., Salmaso, N., 2017. Warming trends of perialpine lakes from homogenised time series of historical satellite and *in-situ* data. Sci. Total Environ. 578, 417–426. https://doi.org/10.1016/j.scitotenv.2016.10.199.
Peeters, F., Straile, D., Lorke, A., Livingstone, D.M., 2007. Earlier onset of the spring phytoplankton bloom in lakes of the temperate zone in a warmer climate. Glob. Change Biol. 13 (9), 1898–1989. https://doi.org/10.1111/j.1365-2486.2007.01412.x.
Poole, H.H., Atkins, W.R.G., 1929. Photo-electric measurements of submarine illumination throughout the year. J. Mar. Biol. Assoc. U.K. 16 (1), 297–324. https://doi.org/10.1017/S0025315400029829.
Reynolds, C.S., 2006. The Ecology of Phytoplankton, third ed. Cambridge University Press, New York.
Rigosi, A., Marcé, R., Escot, C., Rueda, F.J., 2011. A calibration strategy for dynamic succession models including several phytoplankton groups. Environ. Model. Softw. 26 (6), 697–710. https://doi.org/10.1016/j.envsoft.2011.01.007.
Rinke, K., Eder, M., Peeters, F., Kümmerlin, R., Gal, G., Rothhaupt, K.-O., 2009. Simulating phytoplankton community dynamics in Lake Constance with a coupled hydrodynamic-ecological model. Verh. Int. Ver. Theor. Angew. Limnol. 30 (5), 701–704.
Rinke, K., Yeates, P., Rothhaupt, K.-O., 2010. A simulation study of the feedback of phytoplankton on thermal structure via light extinction. Freshwater Biol. 55 (8), 1674–1693. https://doi.org/10.1111/j.1365-2427.2010.02401.x.
Rogora, M., Buzzi, F., Dresti, C., Leoni, B., Lepori, F., Mosello, R., Patelli, M., Salmaso, N., 2018. Climatic effects on vertical mixing and deep-water oxygen content in the subalpine lakes in Italy. Hydrobiologia 824 (1), 33–50. https://doi.org/10.1007/s10750-018-3623-y.
Romero, J.R., Antenucci, J.P., Imberger, J., 2004. One- and three-dimensional biogeochemical simulations of two differing reservoirs. Ecol. Model. 174 (1-2), 143–160. https://doi.org/10.1016/j.ecolmodel.2004.01.005.
Rounsefell, G.A., 1946. Fish production in lakes as a guide for estimating production in proposed reservoirs. Copeia 1946 (1), 29–40. https://doi.org/10.2307/1438819.
Ruggiu, D., Morabito, G., Panzani, P., Pugnetti, A., 1998. Trends and relations among basic phytoplankton characteristics in the course of the long-term oligotrophication of Lake Maggiore (Italy). Hydrobiologia 369/370, 243–257. https://doi.org/10.1023/A:1017058112298.
Salmaso, N., 2005. Effects of climatic fluctuations and vertical mixing on the interannual trophic variability of Lake Garda, Italy. Limnol. Oceanogr. 50 (2), 553–565. https://doi.org/10.4319/lo.2005.50.2.0553.
Salmaso, N., 2010. Long-term phytoplankton community changes in a deep subalpine lake: responses to nutrient availability and climatic fluctuations. Freshwater Biol. 55 (4), 825–846. https://doi.org/10.1111/j.1365-2427.2009.02325.x.
Salmaso, N., Buzzi, F., Cerasino, L., Garibaldi, L., Leoni, B., Morabito, G., Rogora, M., Simona, M., 2014. Influence of atmospheric modes of variability on the limnological characteristics of large lakes south of the Alps: a new emerging paradigm. Hydrobiologia 731 (1), 31–48. https://doi.org/10.1007/s10750-013-1659-6.
Sander, R., 2015. Compilation of Henry's law constants (version 4.0) for water as solvent. Atmos. Chem. Phys. 15, 4399–4981. https://doi.org/10.5194/acp-15-4399-2015.
Schladow, S.G., Hamilton, D.P., 1997. Prediction of water quality in lakes and reservoirs: part II - Model calibration, sensitivity analysis and application. Ecol. Model. 96 (1-3), 111–123. https://doi.org/10.1016/S0304-3800(96)00063-4.
Shimoda, Y., Arhonditsis, G.B., 2016. Phytoplankton functional type modelling: running before we can walk? A critical evaluation of the current state of knowledge. Ecol. Model. 320, 29–43. https://doi.org/10.1016/j.ecolmodel.2015.08.029.
Snortheim, C.A., Hanson, P.C., McMahon, K.D., Read, J.S., Carey, C.C., Dugan, H.A., 2017. Meteorological drivers of hypolimnetic anoxia in a eutrophic, north temperate lake. Ecol. Model. 343, 39–53. https://doi.org/10.1016/j.ecolmodel.2016.10.014.
Stefani, F., Salerno, F., Copetti, D., Rabuffetti, D., Guidetti, L., Torri, G., Naggi, A., Iacomini, M., Morabito, G., Guzzella, L., 2016. Endogenous origin of foams in lakes: a long-term analysis for Lake Maggiore (northern Italy). Hydrobiologia 767 (1), 249–265. https://doi.org/10.1007/s10750-015-2506-8.
Tapolczai, K., Anneville, O., Padisák, J., Salmaso, N., Morabito, G., Zohary, T., Tadonléké, R.D., Rimet, F., 2015. Occurrence and mass development of *Mougeotia* spp. (Zygnemataceae) in large, deep lakes. Hydrobiologia 745 (1), 17–29. https://doi.org/10.1007/s10750-014-2086-z.
Trolle, D., Hamilton, D.P., Hipsey, M.R., et al., 2012. A community-based framework for aquatic ecosystem models. Hydrobiologia 683 (1), 25–34. https://doi.org/10.1007/s10750-011-0957-0.
Trolle, D., Hamilton, D.P., Pilditch, C.A., Duggan, I.C., Jeppesen, E., 2011. Predicting the effects of climate change on trophic status of three morphologically varying lakes: implications for lake restoration and management. Environ. Model. Softw. 26 (4), 354–370. https://doi.org/10.1016/j.envsoft.2010.08.009.
Trolle, D., Jørgensen, T.B., Jeppesen, E., 2008a. Predicting the effects of reduced external nitrogen loading on the nitrogen dynamics and ecological state of deep Lake Ravn, Denmark, using the DYRESM–CAEDYM model. Limnologica 38 (3-4), 220–232. https://doi.org/10.1016/j.limno.2008.05.009.
Trolle, D., Skovgaard, H., Jeppesen, E., 2008b. The Water Framework Directive: setting the phosphorus loading target for a deep lake in Denmark using the 1D lake ecosystem model DYRESM–CAEDYM. Ecol. Model. 219 (1-2), 138–152. https://doi.org/10.1016/j.ecolmodel.2008.08.005.